Fully deprotected β-(1→2)-mannotetraose forms a contorted α-helix in solution: convergent synthesis and conformational characterization by NMR and DFT†

Filip S. Ekholm,[a] Jari Sinkkonen[b] and Reko Leino*[a]

Received (in Montpellier, France) 24th November 2009, Accepted 3rd December 2009
First published as an Advance Article on the web 20th January 2010
DOI: 10.1039/b9nj00702d

β-(1→2)-linked oligomannosides, found in the cell wall of *Candida albicans*, are promising structures for the development of *C. albicans* vaccines. Considerable effort in recent years has been devoted to the synthesis of these carbohydrate structures. As a result, several successful synthetic methodologies based on linear approaches have emerged. Here, we demonstrate that a fully deprotected β-(1→2)-linked mannotetrasaccharide can also be conveniently constructed by the convergent direct coupling of two appropriately protected disaccharides. This improved approach offers several advantages over previously published methods. The number of steps needed to reach larger oligosaccharides is decreased, while high selectivity is retained when the crucial glycosylation step is performed with two disaccharides, herein providing β-(1→2)-mannotetraose in 4.2% overall yield over 16 steps starting from D-mannose. Additionally, the complete structural characterization of the products by NMR spectroscopy is reported. In the conformational study of the final product, 2D-NOESY was used in combination with spectral simulations performed using PERCH software. The experimental results obtained confirm the contorted α-helical structure predicted earlier for these oligosaccharides in solution. As a culmination of the conformational study, a model was constructed by molecular modeling using DFT, and the minimum energy conformation was found to be in full agreement with the experimental results. This is the first study to date where the conformation of a fully deprotected mannotetraose has been reported.

Introduction

The yeast *Candida albicans*, an opportunistic pathogen found in the mucous membrane of the gut, skin, gastrointestinal tract and mouth, is considered to be part of the normal human flora. In immunocompromised patients, *C. albicans* can grow out of control, a condition termed candidiasis, thereby resulting in severe infections.[1] Through studies on the composition of *C. albicans*' cell wall, an epitope consisting of β-(1→2)-linked mannans, isolated from the acid labile fraction of phosphopeptidomannan, was identified as important for the inhibition of such infections.[1c,2] To date, several biological studies have confirmed the protective role of β-(1→2)-linked mannans and furthermore implicated their involvement in the stimulation of TNF-α production from macrophages.[1c,3]

There are several synthetic challenges associated with the construction of β-linked mannosides. Both thermodynamic and kinetic conditions lead to formation of the α-anomer. In addition to these effects, neighbouring group participation from ester protective groups at C-2 will lead to formation of the α-mannoside.[4] Despite this challenge, several successful methodologies have been developed to overcome these difficulties.[4a,5] Although the development of selective methodologies for the synthesis of complex carbohydrates can be considered important, the full spectroscopic analysis of such structures is of equal importance.

The cell wall composition of *C. albicans* has been the subject of several structural studies.[2] Special attention has been drawn to the β-(1→2)-linked mannans, not only due to the immunochemical activity shown by portions of these polymers but also because such structures have been predicted to display interesting conformational properties.[6] Delicate conformational studies by Bundle and colleagues on propyl-capped glycosides have revealed that these carbohydrates form contorted α-helical structures in solution.[6b] Studies on fully deprotected oligomannosides have, however, not been reported previously.

In light of the extensive and elegant work previously carried out in this field, we present here an improved convergent synthetic protocol for the synthesis of β-(1→2)-mannotetraose, in part derived and modified from the earlier linear approaches developed by Crich and Mallet *et al.*, for the synthesis of β-(1→2)-linked oligomannosides.[5d,e] The advantages gained from the enhanced convergent approach presented reduces the number of reaction steps while maintaining a high selectivity in the crucial glycosylation. In addition, the full ^{1}H and ^{13}C NMR spectroscopic analysis and signal assignments of both

[a] *Laboratory of Organic Chemistry, Åbo Akademi University, FI-20500, Åbo, Finland. E-mail: reko.leino@abo.fi; Fax: +358 2-2154866; Tel: +358 2-2154132*
[b] *Laboratory of Organic Chemistry and Chemical Biology, University of Turku, FI-20014, Turku, Finland*

† Electronic supplementary information (ESI) available: Complete spectral data for structures **3** and **4** (in both MeOD and D_2O), along with molecular modelling data for structure **4**. See DOI: 10.1039/b9nj00702d

the protected and deprotected mannotetraoses, including spectral simulations and accurate determinations of coupling constants, are presented here for the first time. The experimental data obtained was further utilized in the conformational analysis of the final product, the minimum energy conformation of which was also verified by molecular modelling using density functional theory.

Results and discussion

Synthesis of β-(1→2)-mannotetraose

Previous work at our laboratory has focused on the synthesis of fully deprotected β-(1→2)-linked mannotriose and some of its close analogues by the utilization of a linear glycosylation strategy.[7] With this protocol, the efficient and highly selective synthesis of β-(1→2)-linked mannosides is accomplished by activation of a thioglycoside (or mannopyranosyl sulfoxide) at low temperatures with 1-(phenylsulfinyl) piperidine (BSP), 2,4,6-tri-*tert*-butyl pyrimidine (TTBP) and Tf_2O, thereby forming an α-D-mannopyranosyl triflate, which in turn reacts with an acceptor in an S_N2 fashion. Further notable features of this method involve the influence of protecting groups, especially the 4,6-*O*-benzylidene acetal, on the outcome of glycosylation.[8] This direct highly β-selective mannosylation protocol, originally developed in the group of Crich, was, in their work, successfully utilized for the synthesis of a cyclohexyl-capped, β-(1→2)-linked mannooctasaccharide.[5e] As noted by Crich and co-workers,[5e] when progressing from the trisaccharide stage towards the tetrasaccharide, a significant decrease in selectivity, from β : α 9.9 : 1 to 3.9 : 1, of the individual coupling reaction is observed. Despite the decrease in selectivity, a high efficiency is maintained throughout the entire synthetic pathway.

Mallet *et al.* earlier reported a convergent approach based on a similar protective group strategy, where two disaccharides were coupled to obtain a tetrasaccharide.[5d] However, in their work, neither the selectivity of the crucial coupling step nor NMR spectroscopic data for the compounds prepared was reported. A major drawback of their approach was the use of three different types of protective groups, requiring a three step deprotection sequence in order to obtain the fully deprotected β-(1→2)-linked mannotetrasaccharide. Another successful approach, developed by Bundle and co-workers, has likewise received considerable attention recently.[5b,5f] The key features of this method consist of glycosylation utilizing a ulosyl donor, followed by epimerization at C-2 with L-selectride. This strategy was successfully applied to the synthesis of β-(1→2)-linked oligomannosides with a degree of polymerization (DP) from two to six.[6b] Despite the high selectivities throughout the synthesis, the yields of the individual glycosylation reactions declined when approaching the tetrasaccharide, from 65% in the trisaccharide step to 48% in the tetrasaccharide step.

Considering the general advantages of the previously reported attempts, we set out to prepare fully deprotected β-(1→2)-mannotetraose by a modified convergent approach. In general, the convergent approach has several advantages over its linear counterpart, the most important being, in most cases, a shortened synthetic route.[9]

The disaccharide building blocks **1** and **2** (Fig. 1) were synthesized according to the slightly modified literature methodologies developed by Crich *et al.* and previously also utilized in our laboratory.[10] The reaction route employed in our previous study for the preparation of donor **1** was shortened by four steps by the direct dibenzylation of phenyl 4,6-*O*-benzylidene-1-thio-α-D-mannopyranoside, followed by a coupling with the thio acceptor at −78 °C, thereby giving disaccharide donor **1** in 76% yield (β : α 9.9 : 1) over two steps. Donor **1** was coupled with acceptor **2** in a similar fashion to obtain protected tetrasaccharide **3** (Scheme 1).[11] After a subsequent work-up and purification, compound **3** was isolated in 55% yield (β : α 10 : 1). In comparison with the earlier reported linear approach,[5e] the selectivity of the crucial glycosylation was more than two times better when the convergent protocol was tested. The yield was only slightly lower than those reported earlier by Crich and co-workers[5e] (53% yield, starting from the disaccharide acceptor and monosaccharide donor) but slightly higher than the yield reported by Bundle *et al.*[5b] (31% yield, starting from the disaccharide acceptor and monosaccharide donor). In contrast with the convergent approach of Mallet *et al.*,[5d] the deprotection of the β-(1→2)-linked mannotetrasaccharide can here be achieved by a one step hydrogenolysis instead of the three step deprotection sequence required by the earlier approach. Therefore, the improved convergent approach developed and utilized in this paper can be considered a feasible alternative when constructing larger β-(1→2)-mannans.

The final deprotection of **3** by hydrogenolysis under 2.8 bar H_2 in methanol proceeded smoothly to provide **4**. The yield was, however, highly dependent on the deprotection conditions. When using 2.5 weight equiv. of Pd/C (10% Pd) with a substrate concentration of 10 mg ml^{-1} methanol, a reduced tetrasaccharide containing mannitol at the reducing end was obtained in 40% yield. The formation of this byproduct was verified by both HRMS (m/z = 691.2281 $[M + Na]^+$) and NMR spectroscopy, showing three anomeric signals in the ^1H NMR spectrum at 4.89, 4.82 and 4.81 ppm, and in the ^{13}C NMR spectrum at 101.1, 100.5 and 99.7 ppm, respectively. Formation of this undesired side-product was, however, strongly suppressed when 2 weight equiv. Pd/C was used and the concentration of **3** was 20 mg ml^{-1} methanol, thereby increasing the yield of the desired product to 75% (for purification details, see the Experimental section).

Characterization by NMR spectroscopy

In order to verify the linkages and fully characterize the products, several NMR spectroscopic methods were utilized.

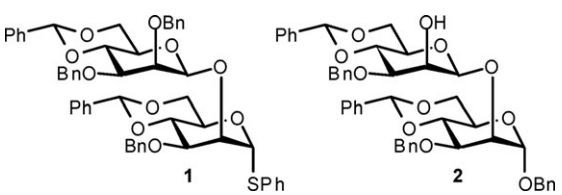

Fig. 1 The disaccharide building blocks **1** and **2**.

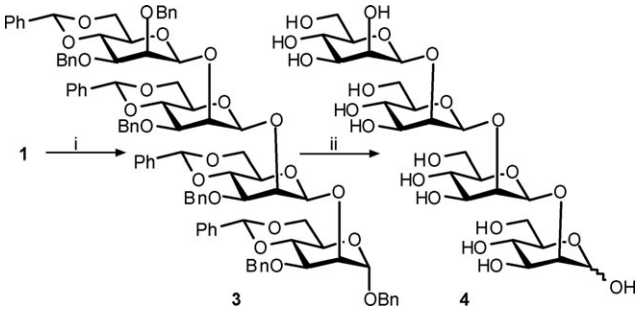

Scheme 1 (i) (a) TTBP, BSP, Tf_2O, CH_2Cl_2, −60 °C, 0.5 h; (b) **2**, −78 °C, 3 h, 55%. (ii) Pd/C, H_2 (2.8 bar), MeOH, rt, 19.5 h, 75%.

In the ^{1}H NMR spectrum of **3**, chemical shifts for the three H-5$_\beta$ protons were observed at low frequencies (3.42 ppm for H-5″, 3.31 ppm for H-5′ and 3.30 ppm for H-5‴) in comparison to the chemical shift of H-5$_\alpha$ (3.86 ppm for H-5), thereby suggesting that the β-anomer was indeed formed. A similar difference was witnessed in the ^{13}C NMR spectrum, where the three C-5$_\beta$ carbons (67.9 ppm for C-5″, 67.8 ppm for C-5′ and 67.5 ppm for C-5‴) appear at a slightly higher frequency than the C-5$_\alpha$ carbon (64.2 ppm for C-5). These results are in accordance with the general view on the chemical shifts of α- and β-mannosides.[5e,7a,12] Furthermore, an upfield shift of the three H-3$_\beta$ protons (3.64 ppm for H-3′, and 3.53 ppm for H-3‴ and H-3″) was observed, further indicating a different linkage to the one existing in the first residue (4.01 ppm for H-3). In addition, the coupling constants obtained by simulation of the ^{1}H NMR spectrum clearly indicated a difference between the H-1–H-2 coupling constants for the α-linked residue ($J_{1,2}$ = 1.6 Hz for H-1) and the β-linked residues ($J_{1'',2''}$ = 0.3 Hz for H-1″, $J_{1''',2'''}$ = 0.8 Hz for H-1‴ and $J_{1',2'}$ = 0.7 Hz for H-1′), providing further support for the assigned stereochemistry. Ultimately, the linkages were proven by the use of coupled HSQC, showing large differences in the $J_{C,H}$ coupling constants ($J_{C\text{-}1''',H\text{-}1'''}$ = 158.3 Hz for C-1‴, $J_{C\text{-}1'',H\text{-}1''}$ = 158.6 Hz for C-1″, $J_{C\text{-}1',H\text{-}1'}$ = 156.0 Hz for C-1′ and $J_{C\text{-}1,H\text{-}1}$ = 167.8 Hz for C-1).

In general, the full spectral characterization of complex oligosaccharides is one of the most demanding tasks in carbohydrate chemistry.[13] For this purpose, 1D-TOCSY (1D-TOtal Correlation SpectroscopY) proved to be a valuable tool.[14] Well separated signals corresponding to the different ring units were targeted by selective excitation, and a spinlock time of 500 ms was found to be suitable for assuring magnetization spreading to the entire ring system.

The use of 1D-TOCSY reduced the spectral complexity to a monosaccharide level. The order of the residues and the positions of the protecting groups were determined by HMBC. The full spectral assignment was finally carried out using PERCH (PEAk ResearCH) NMR software, the results of which are shown in Fig. 2.[15]

In order to fully assign the ^{1}H NMR spectrum of **4**, a similar set of NMR spectroscopic methods were needed. The NMR spectrum of a tetrasaccharide alone is, in many cases, problematic to solve as such. Here, due to mutarotation, an α : β ratio of 7 : 2 for **4** was observed, thereby complicating the assignment even further. Again, 1D-TOCSY proved to be a powerful tool and was utilized to overcome the complications. Compound **4** gave rise to well separated signals corresponding to the H-1 and H-2 protons on the different residues of both anomers. These signals were also targeted with 1D-TOCSY. It was observed that the separation is highly influenced by the NMR solvent used (MeOD *vs.* D_2O). In MeOD, an enhanced separation of the crucial signals was observed. From a biological standpoint, however, D_2O is of more interest and, accordingly, NMR spectroscopic data was recorded in both solvents. The importance of improved signal separation is significant, and thus the following discussion is based on NMR spectra recorded in MeOD. By narrowing the excitation range of the 1D-TOCSY, even signals separated by only 6 Hz were successfully excited to give a ^{1}H NMR spectrum of a single residue. The 1D-TOCSY spectra of all the residues are shown in Fig. 3. To determine the order of the residues, the ^{13}C NMR chemical shifts for the reducing end anomers were chosen as the starting point. These signals appear at a considerably lower frequency (94.1 ppm for C-1α and 95.5 ppm for C-1β) compared to the other anomeric carbons (between 103.3–101.1 ppm). In HMBC, the long range coupling between H-2–C-1′ was clearly visible. The inverse coupling, *i.e.*, H-1′–C-2, was also observed. By iteration of this approach, the different monomers were determined in order, starting from the reducing end residue. H-5‴ was shown to give a signal at a higher frequency in both anomers (3.36 ppm for H-5‴α and 3.39 ppm for H-5‴β) than the remaining H-5$_\beta$ protons (between 3.25–3.20 ppm). This also indicates that the residues were assigned correctly. It was noticed, however, that in D_2O, this effect does not occur, thereby all the H-5$_\beta$ protons appear at a similar chemical shift. Furthermore, the 2D-NOESY spectrum shows correlations through space between H-1$^{n+'}$ and H-2^n (where n = 0, ′ and ″), which are in agreement with the assignment based on the HMBC spectrum. The information gained by 2D-NOESY will be further discussed below when assessing the conformation of this molecule. With the information received from these standard NMR methods (^{1}H, ^{13}C, DQF-COSY, HSQC, HMBC, 1D-TOCSY and 2D-NOESY), the spectrum was simulated using PERCH. In order to simplify matters, the individual 1D-TOCSY spectra were first simulated, followed simulating the complete spectrum, containing both anomers (Fig. 4).

Conformational analysis

The β-(1→2)-linked oligomannosides were first predicted to form interesting 3D structures, contorted structures folding back upon themselves, more than 30 years ago.[6c] The earlier work by Bundle and co-workers on a β-(1→2)-linked mannopentasaccharide revealed these assumptions to be correct.[6b] NOE contacts between non-contiguous residues were witnessed, thus suggesting that a contorted α-helical structure is indeed formed. These studies were, however, conducted on a propyl-capped glycoside instead of a free β-(1→2)-linked oligomannoside. Further evidence of a contorted structure was reported by Crich *et al.*[6a] During the synthesis of an octameric cyclohexyl-capped oligomannoside, they were able to crystallize a fully protected tetrasaccharide. In the present study, the conformational analysis was performed with **4**,

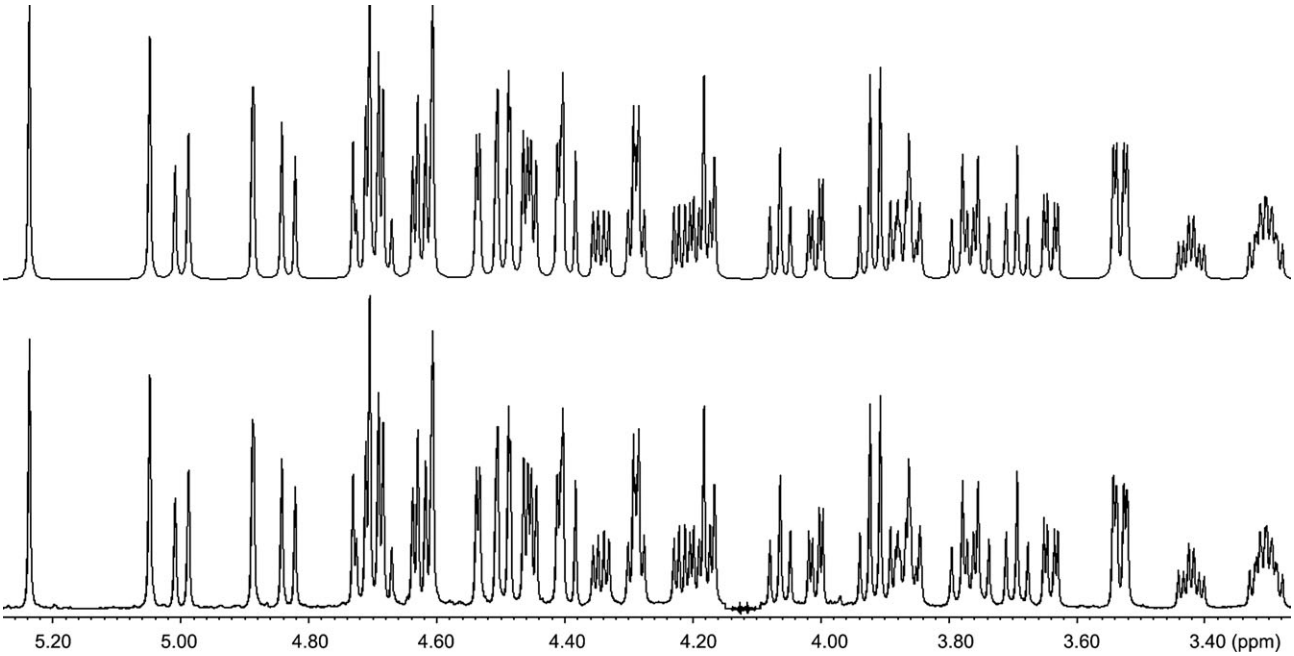

Fig. 2 A spectral simulation of the ^{1}H NMR spectrum of **3** (5.3–3.2 ppm region) using PERCH NMR software; top: simulated spectrum, bottom: observed spectrum.

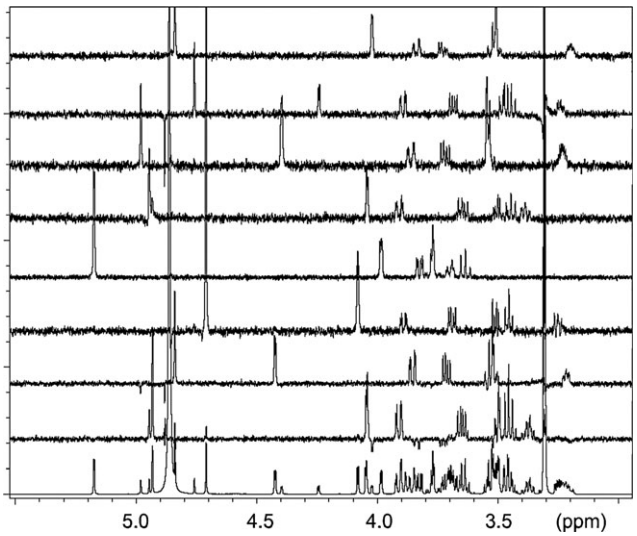

Fig. 3 1D-TOCSY spectra of the different ring units in **4** (in MeOD). From the top: β, β′, β″, β‴, α, α′, α″, α‴ and the entire spectrum.

bearing no protective groups. Therefore, the observed conformation should only result from the steric and electronic interaction displayed by the oligosaccharide itself. In contrast to the previous studies, where β-linked glycosides were used, the discussion below is based on information from the dominating α-anomer.

Luckily, H-4 was well separated (dd at 3.63 ppm) in the ^{1}H NMR spectrum of **4** recorded in MeOD. This was not the case in D_2O. From the 2D-NOESY spectrum, the correlations also witnessed by Bundle and co-workers were confirmed.[6b] The most important correlations, between the non-contiguous residues, are H-4–H-2″, H-4–H-1″ and H-4–H-1‴ (Fig. 5 and Fig. 6). The H-4–H-2″ correlation was, however, stronger than the H-4–H-1″ and H-4–H-1‴ correlations. This information confirms the contorted structure predicted several years ago, and witnessed by Bundle *et al.*[6b] and Crich *et al.*[6a]

In addition, a correlation between H-1–H-1′ and H-1–H-2′ was observed here for the first time. The lack of this correlation in the study performed by Bundle and co-workers may have been partly due to the use of a propyl-capped β-linked mannoglycoside. Furthermore, 2D-NOESY correlations between H-1$^{n+\prime}$ and H-2^{n} (where n = 0, ′ and ″) were witnessed, thereby suggesting steric interactions to place the residues in a specific order. In addition, correlations between H-1–H-2, H-1–H-3 and H-1–H-5 of the β-linked residues, along with the accurate coupling constants obtained using PERCH, suggest the different residues exist in the $^{4}C_1$ chair conformation.

To further investigate and verify the conformation suggested by NMR, computational methods were utilized to model the preferred structure. The initial structure was first sketched by quick modelling using molecular mechanics with Chem3D Pro 11.0 software. The geometry of the achieved structure was further optimized by the DFT method B3LYP using the 6-31G(d,p) basis set. This method has been found to give good results in reasonable time for fairly large molecules.[16] Since the potential energy surface of relatively flexible molecules may consist of several minima, the first attempt did not find the structure that would correspond to all of the NMR spectroscopic (especially NOE) results. Therefore, the torsion angles were modified in order to obtain a starting structure that was in agreement with the observed NOE correlations. When this structure was optimized, a stationary point was found that was in full agreement with the experimental results. Frequency calculations were performed in order to prove that the stationary point found is indeed a minimum energy point. The optimized structure is presented in Fig. 6 and Fig. 7, and is reported in Cartesian coordinates in

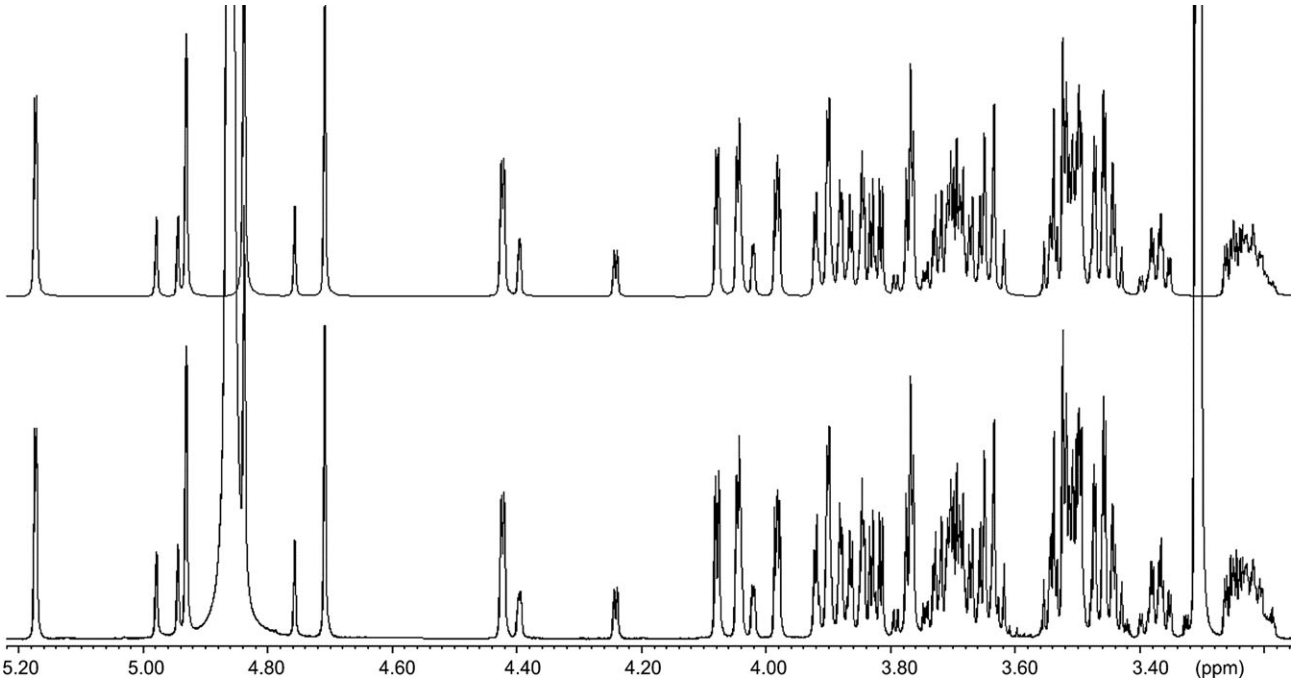

Fig. 4 Spectral simulation of the ^{1}H NMR spectrum of **4** (5.2–3.1 ppm region) using PERCH NMR software; top: simulated spectrum, bottom: observed spectrum.

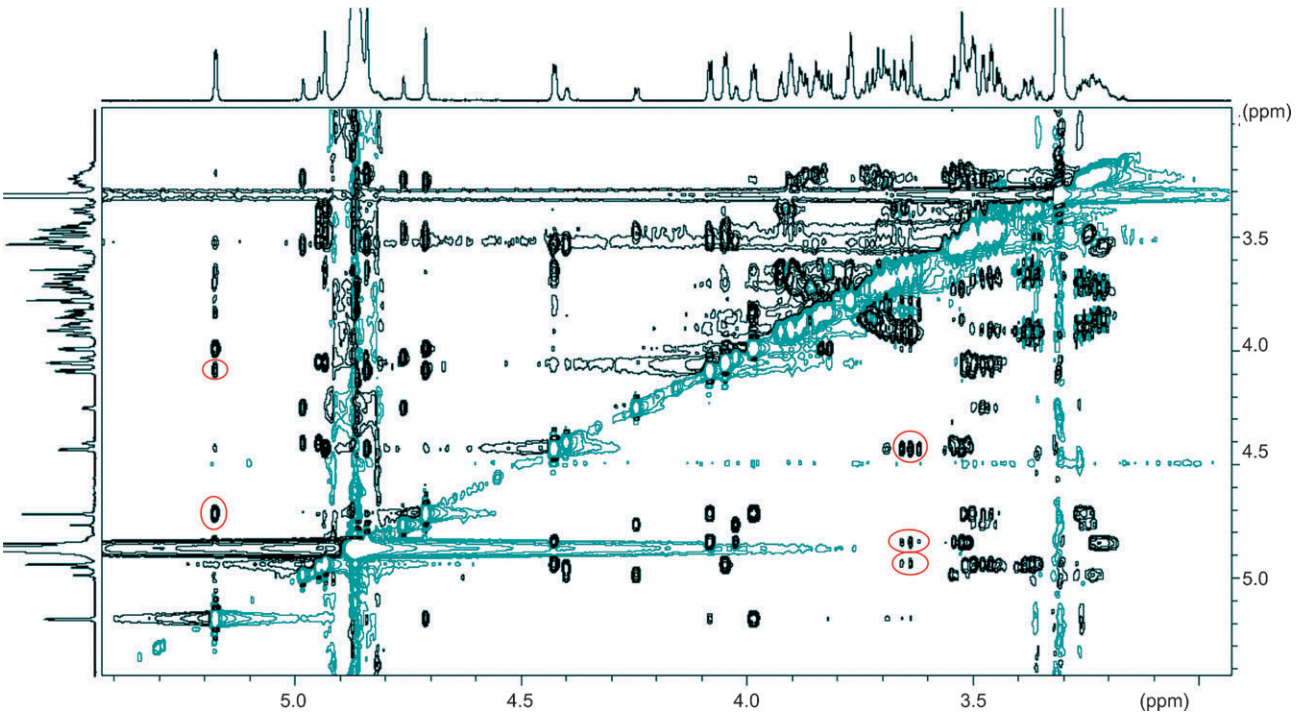

Fig. 5 The 2D-NOESY spectrum of **4** in MeOD, displaying correlations between protons that are close in space. The most important correlations are highlighted with red circles.

the ESI.† The distances between the protons in the optimized structure for the key NOE connectivities were found to be 3.19 Å (H-4–H-2″), 4.13 Å (H-4–H-1″) and 3.65 Å (H-4–H-1‴). These results were in good agreement with the peak intensities witnessed in the NOESY spectrum. All of the mannose moieties were found to exist in the $^{4}C_{1}$ conformation as expected. The optimized results also exhibit the contorted α-helical structure of the molecule (Fig. 7).

It was previously suggested that the glycosidic linkages are hidden in the middle of the contorted α-helical structure, thus creating a hydrophobic interior, and that the hydroxyl groups are oriented outwards, further creating a hydrophilic

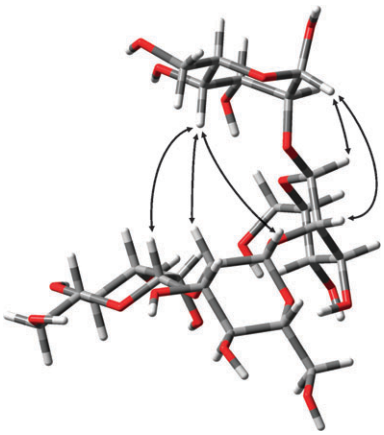

Fig. 6 The B3LYP/6-31G(d,p) optimized structure of the α-anomer, showing the most important NOESY correlations.

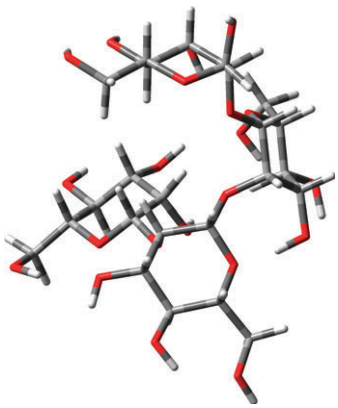

Fig. 7 The B3LYP/6-31G(d,p) optimized structure of the α-anomer, displaying the contorted α-helical nature of the molecule.

exterior.[6b] A similar pattern can be witnessed for the fully deprotected tetrasaccharide, as displayed in Fig. 7. These structures may have increased stability towards hydrolysis as the glycosidic bonds are hidden in the middle of the helix. Due to the helical nature of these molecules, they could be used in the site selective modification of proteins to insert helical fragments of well defined structure (as a structural motif) into a protein backbone.[17]

Conclusions

To summarize, an improved protocol for the synthesis of β-(1→2)-linked oligomannosides has been developed and utilized in the synthesis of a fully deprotected β-(1→2)-mannotetraose. The key features of this method involve a crucial coupling being performed between a disaccharide donor and acceptor. A careful design strategy for the protective group allows the deprotection to be carried out in one step. Furthermore, NMR spectroscopic methods widely applicable to the characterization of complex oligosaccharides were investigated and presented in detail. These methods were utilized in the full spectroscopic assignment and accurate determination of coupling constants for both the protected and deprotected mannan tetrasaccharides. In addition, the first conformational study and complete NMR spectroscopic characterization of a fully deprotected β-(1→2)-linked mannotetrasaccharide was executed based on the information obtained from different NMR spectroscopic techniques. By using molecular modelling, a model in good agreement with the experimental results was obtained, thereby providing further evidence of the conformation adopted by these molecules in solution. The NMR spectroscopic information presented here will, in the future, be used as a starting point when studying interactions between **4** and receptors on macrophages. This could potentially provide information about the crucial functionalities needed for binding to the receptor and may result in the development of simpler structures for *C. albicans* vaccines.

Experimental section

Instrumentation and general experimental details

Reaction solvents were dried and distilled prior to use when necessary. All reactions containing moisture or air sensitive reagents were carried out under an argon atmosphere.

NMR spectra were recorded using Bruker Avance NMR spectrometers operating at 500.13 MHz (^{1}H: 500.13 MHz, ^{13}C: 125.77 MHz) or 600.13 MHz (^{1}H: 600.13 MHz, ^{13}C: 150.90 MHz). Both spectrometers had a similar basic configuration with a lock channel (^{2}H), and a high frequency (^{1}H–^{19}F) and broad band frequency channel (^{109}Ag–^{31}P). Both instruments were equipped with a Z gradient facility and carried inverse double resonance probes with a Z-axis gradient. Each spectrometer had two waveform generators for work with shaped pulses. The probe temperature during the experiments was kept at 25 °C. All products were fully characterized by utilizing ^{1}H, ^{13}C and TOCSY 1D techniques, in combination with DQF-COSY, NOESY, HSQC (both coupled and decoupled) and HMBC 2D techniques, by using pulse sequences provided by the manufacturer.

^{1}H NMR spectra were acquired using the *zg30* pulse program with spectral widths of 12 kHz consisting of 64 K data points zero-filled to 256 K prior to Fourier transformation. A single-pulse excitation with a 30° flip angle was used. ^{13}C NMR spectra were acquired using the *zgpg30* pulse program with spectral widths of 36 kHz consisting of 65 K data points zero-filled to 128 K prior to Fourier transformation. A single-pulse excitation with a 30° flip angle was used. Furthermore, an exponential window function was used when processing the FID (lb 1 Hz). TOCSY 1D spectra were acquired using either the *selmlzf* or *selmlgp.2* pulse program with a spin lock time of 500–700 ms. Spectral widths of 10–12 kHz consisting of 32 K data points zero-filled to 64 K prior to FFT. Gradient versions of the 2D techniques were used. DQF-COSY spectra were measured using the *cosygpmfqf* pulse program. HSQC spectra were measured using the *hsqcetgpsi* pulse program. In order to obtain $^{1}J_{C,H}$ coupling constants, the decoupling pulse power was turned to zero (120 dB), resulting in a proton-coupled HSQC spectrum. HMBC spectra were acquired using the *hmbcgplpndqf* pulse program with $^{1}J_{H,C}$ = 145 Hz and $^{n}J_{H,C}$ = 2–10 Hz. NOESY 2D spectra were acquired using the *noesygpph* pulse program with a mixing time between 0.5–1.0 s.

Chemical shifts are expressed on the δ scale (in ppm) using TMS (tetramethylsilane), residual chloroform, acetone, H_2O or methanol as internal standards. Coupling constants are given in Hz and coupling patterns are given as s: singlet, d: doublet, t: triplet, *etc*. When signals appear at similar chemical shifts, if possible, additional decimals are used to determine the order of the signals. Computational analysis of the ^{1}H NMR spectra of compounds **3** and **4** was achieved using PERCH NMR software, with starting values and spectral parameters obtained from the various NMR techniques used.[15]

HRMS were recorded using a Bruker Micro Q-TOF instrument with ESI (electrospray ionization) operating in positive mode. Optical rotations were measured at 23 °C with a Perkin-Elmer polarimeter equipped with a sodium lamp (589 nm). TLC was performed on aluminium sheets pre-coated with silica gel 60 F_{254} (Merck). Preparative TLC was performed on aluminium sheets pre-coated with silica gel 60 F_{254} (0.5 cm, Merck). Flash chromatography was carried out on silica gel 60 (0.040–0.060 mm, Merck). Spots were visualized by UV, followed by charring with 1 : 10 H_2SO_4 : MeOH and heating. Compound **4** was purified by high-pH anion exchange chromatography (HPAEC) using a Dionex DX600 system equipped with an amperometric detector.

The initial structure for modelling was drawn using ChemBioDraw Ultra 11.0 and modelled by Chem3D Pro 11.0 using a MM2 molecular mechanics method. All higher quality calculations were performed by Gaussian 03 software using the density functional method B3LYP as a hybrid functional and 6-31G(d,p) as the basis set.[18] The results were examined using the GaussView 4.1.2 program.

Synthetic procedures

Benzyl 2,3-di-*O*-benzyl-4,6-*O*-benzylidene-β-D-mannopyranosyl-(1→2)-3-*O*-benzyl-4,6-*O*-benzylidene-β-D-mannopyranosyl-(1→2)-3-*O*-benzyl-4,6-*O*-benzylidene-β-D-mannopyranosyl-(1→2) -3-*O*-benzyl-4,6-*O*-benzylidene-α-D-mannopyranoside (3). To a solution containing **1** (76 mg, 0.086 mmol) in dry dichloromethane (2.5 ml) was added at −60 °C (acetone + dry ice) BSP (22 mg, 0.10 mmol, 1.2 equiv.), TTBP (32 mg, 0.13 mmol, 1.5 equiv.) and Tf_2O (19 µl, 0.12 mmol, 1.3 equiv.). The resulting mixture was stirred for 0.5 h, followed by cooling to −78 °C and the addition of **2** (78 mg, 0.10 mmol, 1.15 equiv.) dissolved in dichloromethane (1.5 ml) over a time period of 15 min. The reaction mixture was stirred for 2 h and quenched by the addition of triethylphosphite (68 µl). The reaction mixture was then stirred for 1 h at −78 °C, brought to RT, diluted with dichloromethane (30 ml) and washed with a saturated $NaHCO_3$ solution. The water phase was separated and extracted with dichloromethane (3 × 20 ml). The combined organic phase was washed with brine (30 ml), dried with Na_2SO_4, filtered and concentrated. The crude product was purified by preparative TLC (hexane : ethyl acetate 3 : 2). The spots containing the product were scraped off the plate and dissolved in EtOAc (50 ml). After 2 h of stirring, the mixture was filtered and concentrated to give the title compound as a colorless oil (73 mg, β : α 10 : 1, 55%).

TLC: R_f = 0.40 (hexane : ethyl acetate 3 : 2). $[\alpha]_D$ = −25.4 (*c*, 0.5, $CHCl_3$).

^{1}H NMR (600.13 MHz, $CDCl_3$, 25 °C): δ = 7.48–7.07 (m, 50 H, Ar-H), 5.57 (s, 1 H, C*H*‴Ph), 5.52 (s, 1 H, C*H*Ph), 5.43 (s, 1 H, C*H*′Ph), 5.41 (s, 1 H, C*H*″Ph), 5.24 (d, 1 H, $J_{1'',2''}$ = 0.3 Hz, H-1″), 5.05 (d, 1 H, $J_{1''',2'''}$ = 0.8 Hz, H-1‴), 5.00 and 4.83 (each d, each 1 H, J = −12.5 Hz, 2‴-CH_2Ph), 4.89 (d, 1 H, $J_{1,2}$ = 1.6 Hz, H-1), 4.72 and 4.495 (each d, each 1 H, J = −11.9 Hz, 1-CH_2Ph), 4.71 and 4.68 (each d, each 1 H, J = −12.4 Hz, 3-CH_2Ph), 4.69 and 4.62 (each d, each 1 H, J = −12.3 Hz, 3′-CH_2Ph), 4.63 and 4.45 (each d, each 1 H, J = −12.0 Hz, 3″-CH_2Ph), 4.496 and 4.39 (each d, each 1 H, J = −11.8 Hz, 3‴-CH_2Ph), 4.61 (d, 1 H, $J_{1',2'}$ = 0.7 Hz, H-1′), 4.53 (dd, 1 H, $J_{1'',2''}$ = 0.3 Hz, $J_{2'',3''}$ = 3.1 Hz, H-2″), 4.45 (dd, 1 H, $J_{1',2'}$ = 0.7 Hz, $J_{2',3'}$ = 3.2 Hz, H-2′), 4.41 (dd, 1 H, $J_{1''',2'''}$ = 0.8 Hz, $J_{2''',3'''}$ = 3.2 Hz, H-2‴), 4.34 (dd, 1 H, $J_{5'',6''a}$ = 4.7 Hz, $J_{6''a,6''b}$ = −10.2 Hz, H-6″a), 4.29 (dd, 1 H, $J_{1,2}$ = 1.6 Hz, $J_{2,3}$ = 3.5 Hz, H-2), 4.29 (dd, 1 H, $J_{5',6'a}$ = 4.7 Hz, $J_{6'a,6'b}$ = −10.3 Hz, H-6′a), 4.22 (dd, 1 H, $J_{5,6a}$ = 4.8 Hz, $J_{6a,6b}$ = −10.3 Hz, H-6a), 4.182 (dd, 1 H, $J_{4''',5'''}$ = 9.3 Hz, $J_{3''',4'''}$ = 9.8 Hz, H-4‴), 4.177 (dd, 1 H, $J_{5''',6'''a}$ = 4.7 Hz, $J_{6'''a,6'''b}$ = −10.3 Hz, H-6‴a), 4.06 (dd, 1 H, $J_{4'',5''}$ = 9.5 Hz, $J_{3'',4''}$ = 9.6 Hz, H-4″), 4.01 (dd, 1 H, $J_{2,3}$ = 3.5 Hz, $J_{3,4}$ = 10.0 Hz, H-3), 3.92 (dd, 1 H, $J_{4,5}$ = 9.5 Hz, $J_{3,4}$ = 10.0 Hz, H-4), 3.91 (dd, 1 H, $J_{4',5'}$ = 9.4 Hz, $J_{3',4'}$ = 9.9 Hz, H-4′), 3.864 (ddd, 1 H, $J_{5,6a}$ = 4.8 Hz, $J_{4,5}$ = 9.5 Hz, $J_{5,6b}$ = 10.3 Hz, H-5), 3.862 (dd, 1 H, $J_{5''',6'''b}$ = 10.3 Hz, $J_{6'''a,6'''b}$ = −10.3 Hz, H-6‴b), 3.78 (dd, 1 H, $J_{5'',6''b}$ = 10.0 Hz, $J_{6''a,6''b}$ = −10.2 Hz, H-6″b), 3.75 (dd, 1 H, $J_{5',6'b}$ = 10.1 Hz, $J_{6'a,6'b}$ = −10.3 Hz, H-6′b), 3.69 (dd, 1 H, $J_{5,6b}$ = 10.3 Hz, $J_{6a,6b}$ = −10.3 Hz, H-6b), 3.64 (dd, 1 H, $J_{2',3'}$ = 3.2 Hz, $J_{3',4'}$ = 9.9 Hz, H-3′), 3.53 (dd, 1 H, $J_{2''',3'''}$ = 3.2 Hz, $J_{3''',4'''}$ = 9.8 Hz, H-3‴), 3.53 (dd, 1 H, $J_{2'',3''}$ = 3.1 Hz, $J_{3'',4''}$ = 9.6 Hz, H-3″), 3.42 (ddd, 1 H, $J_{5'',6''a}$ = 4.7 Hz, $J_{4'',5''}$ = 9.5 Hz, $J_{5'',6''b}$ = 10.0 Hz, H-5″), 3.31 (ddd, 1 H, $J_{5',6'a}$ = 4.7 Hz, $J_{4',5'}$ = 9.9 Hz, $J_{5',6'b}$ = 10.1 Hz, H-5′) and 3.30 (ddd, 1 H, $J_{5''',6'''a}$ = 4.7 Hz, $J_{4''',5'''}$ = 9.3 Hz, $J_{5''',6'''b}$ = 10.3 Hz, H-5‴) ppm.

^{13}C NMR (150.90 MHz, $CDCl_3$, 25 °C): δ = 139.4–126.1 (Ar-C), 103.5 (C-1‴, $J_{C\text{-}1''',H\text{-}1'''}$ = 158.3 Hz), 101.91 (*C*HPh), 101.88 (*C*′HPh), 101.87 (C-1″, $J_{C\text{-}1'',H\text{-}1''}$ = 158.6 Hz), 101.5 (*C*″HPh), 101.2 (*C*‴HPh), 100.2 (C-1′, $J_{C\text{-}1',H\text{-}1'}$ = 156.0 Hz), 96.9 (C-1, $J_{C\text{-}1,H\text{-}1}$ = 167.8 Hz), 79.0 (C-3‴, C-4), 78.5 (C-4′), 78.3 (C-4‴), 78.2 (C-4″), 76.9 (C-3″), 76.34 (C-3′), 76.27 (C-2″), 75.9 (C-2‴), 74.8 (C-2), 74.63 (2‴-*C*H_2Ph), 74.60 (C-3), 74.2 (C-2′), 72.2 (3-*C*H_2Ph), 72.1 (3‴-*C*H_2Ph), 71.2 (3′-*C*H_2Ph), 70.8 (3″-*C*H_2Ph), 69.5 (1-*C*H_2Ph), 68.87 (C-6″), 68.85 (C-6), 68.72 (C-6‴), 68.66 (C-6′), 67.9 (C-5″), 67.8 (C-5′), 67.5 (C-5‴) and 64.2 (C-5) ppm.

HRMS: *m*/*z* calc. for $C_{94}H_{95}O_{21}Na$ $[M + Na]^+$ 1582.6264; found 1582.6207. *m*/*z* calc. for $C_{94}H_{95}O_{21}K$ $[M + K]^+$ 1598.6003; found 1598.5932.

β-D-Mannopyranosyl-(1→2)-β-D-mannopyranosyl-(1→2)-β-D-mannopyranosyl-(1→2)-D-mannopyranose (4). To a solution containing **3** (0.1 g, 0.064 mmol) in dry MeOH (5.5 ml) was added Pd/C (10% Pd, 0.2 g, 2 weight equiv.). The reaction mixture was placed inside a reactor and the H_2 pressure set to 2.8 bar (40 psi). After 19.5 h, the reaction mixture was diluted with MeOH (3 ml), filtered through Celite and concentrated. The crude product was purified by HPAEC (CarboPac PA 1 column; 9 mm × 250 mm) with the following gradient

elution: 50 mM NaOH over 0–10 min, followed by a linear gradient from 50 to 150 mM NaOH over 10–30 min and finally a linear gradient from 0 to 200 mM NaOAc in 150 mM NaOH over 30–60 min. The product was collected and the fractions neutralized by the addition of 1 M aqueous acetic acid. The sample was de-salted using a column of successive cation and anion exchange resins (Bio-Rad AG 50W-8X Resin 200–400 mesh, hydrogen form and Bio-Rad AG 1-X8 Resin 200–400 mesh, acetate form), and concentrated to give the title compound (32 mg, β : α 7 : 2, 75%).

Data for the α-anomer. ^{1}H NMR (600.13 MHz, CD_3OD, 25 °C): δ = 5.17 (d, 1 H, $J_{1,2}$ = 1.8 Hz, H-1), 4.93 (d, 1 H, $J_{1''',2'''}$ = 0.9 Hz, H-1′′′), 4.84 (d, 1 H, $J_{1'',2''}$ = 0.8 Hz, H-1′′), 4.71 (d, 1 H, $J_{1',2'}$ = 0.7 Hz, H-1′), 4.42 (dd, 1 H, $J_{1'',2''}$ = 0.8 Hz, $J_{2'',3''}$ = 3.1 Hz, H-2′′), 4.08 (dd, 1 H, $J_{1',2'}$ = 0.7 Hz, $J_{2',3'}$ = 2.8 Hz, H-2′), 4.04 (dd, 1 H, $J_{1''',2'''}$ = 0.9 Hz, $J_{2''',3'''}$ = 3.1 Hz, H-2′′′), 3.98 (dd, 1 H, $J_{1,2}$ = 1.8 Hz, $J_{2,3}$ = 3.1 Hz, H-2), 3.91 (dd, 1 H, $J_{5''',6'''a}$ = 2.2 Hz, $J_{6'''a,6'''b}$ = −12.2 Hz, H-6′′′a), 3.89 (dd, 1 H, $J_{5',6'a}$ = 2.3 Hz, $J_{6'a,6'b}$ = −12.0 Hz, H-6′a), 3.85 (dd, 1 H, $J_{5'',6''a}$ = 2.5 Hz, $J_{6''a,6''b}$ = −11.7 Hz, H-6′′a), 3.82 (dd, 1 H, $J_{2,3}$ = 3.1 Hz, $J_{3,4}$ = 9.6 Hz, H-3), 3.78 (dd, 1 H, $J_{5,6b}$ = 4.1 Hz, $J_{6a,6b}$ = −12.0 Hz, H-6b), 3.76 (dd, 1 H, $J_{5,6a}$ = 2.2 Hz, $J_{6a,6b}$ = −12.0 Hz, H-6a), 3.71 (dd, 1 H, $J_{5'',6''b}$ = 5.8 Hz, $J_{6''a,6''b}$ = −11.7 Hz, H-6′′b), 3.70 (ddd, 1 H, $J_{5,6a}$ = 2.2 Hz, $J_{5,6b}$ = 4.1 Hz, $J_{4,5}$ = 9.7 Hz, H-5), 3.69 (dd, 1 H, $J_{5',6'b}$ = 5.8 Hz, $J_{6'a,6'b}$ = −12.0 Hz, H-6′b), 3.65 (dd, 1 H, $J_{5''',6'''b}$ = 7.3 Hz, $J_{6'''a,6'''b}$ = −12.2 Hz, H-6′′′b), 3.63 (dd, 1 H, $J_{3,4}$ = 9.6 Hz, $J_{4,5}$ = 9.7 Hz, H-4), 3.53 (dd, 1 H, $J_{3'',4''}$ = 9.5 Hz, $J_{4'',5''}$ = 9.7 Hz, H-4′′), 3.52 (dd, 1 H, $J_{2'',3''}$ = 3.1 Hz, $J_{3'',4''}$ = 9.5 Hz, H-3′′), 3.51 (dd, 1 H, $J_{2',3'}$ = 2.8 Hz, $J_{3',4'}$ = 9.7 Hz, H-3′), 3.50 (dd, 1 H, $J_{2''',3'''}$ = 3.1 Hz, $J_{3''',4'''}$ = 9.5 Hz, H-3′′′), 3.46 (dd, 1 H, $J_{4''',5'''}$ = 9.2 Hz, $J_{3''',4'''}$ = 9.5 Hz, H-4′′′), 3.45 (dd, 1 H, $J_{4',5'}$ = 9.3 Hz, $J_{3',4'}$ = 9.7 Hz, H-4′), 3.37 (ddd, 1 H, $J_{5''',6'''a}$ = 2.2 Hz, $J_{5''',6'''b}$ = 7.3 Hz, $J_{4''',5'''}$ = 9.2 Hz, H-5′′′), 3.25 (ddd, 1 H, $J_{5',6'a}$ = 2.3 Hz, $J_{5',6'b}$ = 5.8 Hz, $J_{4',5'}$ = 9.3 Hz, H-5′) and 3.21 (ddd, 1 H, $J_{5'',6''a}$ = 2.5 Hz, $J_{5'',6''b}$ = 5.8 Hz, $J_{4'',5''}$ = 9.7 Hz, H-5′′) ppm.

^{13}C NMR (150.90 MHz, CD_3OD, 25 °C): δ = 103.3 (C-1′′), 102.3 (C-1′′′), 101.1 (C-1′), 94.1 (C-1), 81.8 (C-2′), 81.5 (C-2), 79.1 (C-2′′), 78.3 (C-5′, C-5′′), 78.1 (C-5′′′), 75.2 (C-3′′′), 74.3 (C-3′′), 74.2 (C-5), 74.1 (C-3′), 72.1 (C-2′′′), 71.2 (C-3), 69.1 (C-4, C-4′′′), 69.0 (C-4′), 68.6 (C-4′′), 63.5 (C-6′′′), 62.5 (C-6′, C-6′′) and 62.3 (C-6) ppm.

Data for the β-anomer. ^{1}H NMR (600.13 MHz, CD_3OD, 25 °C): δ = 4.98 (d, 1 H, $J_{1'',2''}$ = 0.8 Hz, H-1′′), 4.94 (d, 1 H, $J_{1''',2'''}$ = 1.0 Hz, H-1′′′), 4.84 (d, 1 H, $J_{1,2}$ = 0.8 Hz, H-1), 4.76 (d, 1 H, $J_{1',2'}$ = 0.7 Hz, H-1′), 4.40 (dd, 1 H, $J_{1'',2''}$ = 0.8 Hz, $J_{2'',3''}$ = 2.3 Hz, H-2′′), 4.24 (d, 1 H, $J_{1',2'}$ = 0.7 Hz, $J_{2',3'}$ = 3.2 Hz, H-2′), 4.04 (dd, 1 H, $J_{1''',2'''}$ = 1.0 Hz, $J_{2''',3'''}$ = 2.6 Hz, H-2′′′), 4.02 (dd, 1 H, $J_{1,2}$ = 0.8 Hz, $J_{2,3}$ = 2.4 Hz, H-2), 3.91 (dd, 1 H, $J_{5''',6'''a}$ = 2.4 Hz, $J_{6'''a,6'''b}$ = −12.3 Hz, H-6′′′a), 3.89 (dd, 1 H, $J_{5',6'a}$ = 2.3 Hz, $J_{6'a,6'b}$ = −11.8 Hz, H-6′a), 3.86 (dd, 1 H, $J_{5'',6''a}$ = 2.5 Hz, $J_{6''a,6''b}$ = −11.9 Hz, H-6′′a), 3.83 (dd, 1 H, $J_{5,6a}$ = 2.1 Hz, $J_{6a,6b}$ = −12.1 Hz, H-6a), 3.73 (dd, 1 H, $J_{5,6b}$ = 5.3 Hz, $J_{6a,6b}$ = −12.1 Hz, H-6b), 3.72 (dd, 1 H, $J_{5'',6''b}$ = 5.9 Hz, $J_{6''a,6''b}$ = −11.9 Hz, H-6′′b), 3.68 (dd, 1 H, $J_{5',6'b}$ = 6.2 Hz, $J_{6'a,6'b}$ = −11.8 Hz, H-6′b), 3.65 (dd, 1 H, $J_{5''',6'''b}$ = 7.4 Hz, $J_{6'''a,6'''b}$ = −12.3 Hz, H-6′′′b), 3.54 (dd, 1 H, $J_{2'',3''}$ = 2.3 Hz, $J_{3'',4''}$ = 9.5 Hz, H-3′′), 3.53 (dd, 1 H, $J_{3'',4''}$ = 9.5 Hz, $J_{4'',5''}$ = 9.5 Hz, H-4′′), 3.52 (dd, 1 H, $J_{3,4}$ = 9.7 Hz, $J_{4,5}$ = 9.7 Hz, H-4), 3.50 (dd, 1 H, $J_{2,3}$ = 2.4 Hz, $J_{3,4}$ = 9.7 Hz, H-3), 3.50 (dd, 1 H, $J_{2''',3'''}$ = 2.6 Hz, $J_{3''',4'''}$ = 9.0 Hz, H-3′′′), 3.48 (dd, 1 H, $J_{2',3'}$ = 3.2 Hz, $J_{3',4'}$ = 9.7 Hz, H-3′), 3.45 (dd, 1 H, $J_{3',4'}$ = 9.7 Hz, $J_{4',5'}$ = 9.7 Hz, H-4′), 3.44 (dd, 1 H, $J_{4''',5'''}$ = 8.9 Hz, $J_{3''',4'''}$ = 9.0 Hz, H-4′′′), 3.39 (ddd, 1 H, $J_{5''',6'''a}$ = 2.4 Hz, $J_{5''',6'''b}$ = 7.4 Hz, $J_{4''',5'''}$ = 8.9 Hz, H-5′′′), 3.24 (ddd, 1 H, $J_{5',6'a}$ = 2.3 Hz, $J_{5',6'b}$ = 6.2 Hz, $J_{4',5'}$ = 9.7 Hz, H-5′), 3.23 (ddd, 1 H, $J_{5'',6''a}$ = 2.5 Hz, $J_{5'',6''b}$ = 5.9 Hz, $J_{4'',5''}$ = 9.5 Hz, H-5′′) and 3.20 (ddd, 1 H, $J_{5,6a}$ = 2.1 Hz, $J_{5,6b}$ = 5.3 Hz, $J_{4,5}$ = 9.7 Hz, H-5) ppm.

^{13}C NMR (150.90 MHz, CD_3OD, 25 °C): δ = 103.3 (C-1′′), 103.0 (C-1′), 102.3 (C-1′′′), 95.5 (C-1), 82.3 (C-2), 81.5 (C-2′), 79.1 (C-2′′), 78.4 and 78.3 (C-5, C-5′, C-5′′), 78.0 (C-5′′′), 75.2 (C-3′′′), 74.3 (C-3′, C-3′′), 74.2 (C-3), 72.1 (C-2′′′), 69.1 (C-4′, C-4′′′), 68.8 (C-4), 68.6 (C-4′′), 63.6 (C-6′′′) and 62.6 (C-6, C-6′, C-6′′) ppm.

HRMS: *m*/*z* calc. for $C_{24}H_{24}O_{21}Na$ $[M + Na]^+$ 689.2111; found 689.2131.

Acknowledgements

Financial support from the Academy of Finland (projects #121334 and #121335) is gratefully acknowledged. The authors thank Markku Reunanen (Åbo Akademi University) for HRMS analyses and Dr Jari Helin (Glykos Finland Ltd) for the purification of compound **4**. We also thank Dr Johannes Savolainen, Kaisa Nieminen and Kaarina Ranta (University of Turku), Mattias U. Roslund (Orion Pharma), and Jonas Forsman (Åbo Akademi University) for fruitful discussions.

References

1 See, for example: (*a*) M. Martinez-Esparza, A. Sarazin, N. Jouy, D. Poulain and T. Jouault, *J. Immunol. Methods*, 2006, **314**, 90–102; (*b*) F. Dalle, T. Jouault, P. A. Trinel, J. Esnault, J. M. Mallet, P. d'Athis, D. Poulain and A. Bonnin, *Infect. Immun.*, 2003, **71**, 7061–7068; (*c*) J. Masuoka, *Clin. Microbiol. Rev.*, 2004, **17**, 281–310; (*d*) M. B. Edmond, S. E. Wallace, D. K. McClish, M. A. Pfaller, R. N. Jones and R. P. Wenzel, *Clin. Infect. Dis.*, 1999, **142**, 2741–2746; (*e*) V. J. Fraser, M. Jones, J. Dunkel, S. Storfer, G. Medoff and W. C. Dunagan, *Clin. Infect. Dis.*, 1992, **15**, 414–421.

2 (*a*) N. Shibata, A. Suzuki, H. Kobayashi and Y. Okawa, *Biochem. J.*, 2007, **404**, 365–372; (*b*) H. Kobayashi, H. Oyamada, N. Iwadate, H. Suzuki, H. Mitobe, K. Takahashi, N. Shibata, S. Suzuki and Y. Okawa, *Arch. Microbiol.*, 1998, **169**, 188–194; (*c*) N. Shibata, M. Arai, E. Haga, T. Kikuchi, M. Najima, T. Satoh, H. Kobayashi and S. Suzuki, *Infect. Immun.*, 1992, **60**, 4100–4110; (*d*) H. Kobayashi, N. Shibata, H. Mitobe, Y. Ohkubo and S. Suzuki, *Arch. Biochem. Biophys.*, 1989, **272**, 364–375.

3 See, for example: (*a*) T. Jouault, A. Bernigaud, G. Lepage, P. A. Trinel and D. Poulain, *Immunology*, 1994, **83**, 268–273; (*b*) A. Louie, A. L. Baltch, R. P. Smith, A. M. Franke, W. J. Ritz and J. K. Singh, *Infect. Immun.*, 1994, **62**, 2761–2772; (*c*) T. Jouault, G. Lepage, A. Bernigaud, P. A. Trinel, C. Fradin, J.-M. Wieruszeski, G. Strecker and D. Poulain, *Infect. Immun.*, 1995, **63**, 2378–2381.

4 For a review, see: (*a*) J. J. Gridley and H. M. I. Osborn, *J. Chem. Soc., Perkin Trans. 1*, 2000, 1471–1491; (*b*) S. C. Ennis and H. M.

I. Osborn, in *Carbohydrates*, ed. H. M. I. Osborn, Academic Press–Elsevier, Oxford, 2003, pp. 239–276.
5 See, for example: (*a*) F. Barresi and O. Hindsgaul, *Can. J. Chem.*, 1994, **72**, 1447–1465; (*b*) M. Nitz, B. W. Purse and D. R. Bundle, *Org. Lett.*, 2000, **2**, 2939–2942; (*c*) J. D. C. Codée, L. Kröck, B. Castagner and P. H. Seeberger, *Chem.–Eur. J.*, 2008, **14**, 3987–3994; (*d*) F. Dromer, R. Chevalier, B. Sendid, L. Improvisi, T. Jouault, R. Robert, J. M. Mallet and D. Poulain, *Antimicrob. Agents Chemother.*, 2002, **46**, 3869–3876; (*e*) D. Crich, A. Banerjee and Q. J. Yao, *J. Am. Chem. Soc.*, 2004, **126**, 14930–14934; (*f*) M. Nitz and D. R. Bundle, *J. Org. Chem.*, 2001, **66**, 8411–8423; (*g*) F. Mathew, M. Mach, K. C. Hazen and B. Fraser-Reid, *Synlett*, 2003, 1319–1322.
6 (*a*) D. Crich, H. Li, Q. Yao, D. J. Wink, D. R. Sommer and A. L. Rheingold, *J. Am. Chem. Soc.*, 2001, **123**, 5826–5828; (*b*) M. Nitz, C. C. Ling, A. Otter, J. E. Cutler and D. R. Bundle, *J. Biol. Chem.*, 2002, **277**, 3440–3446; (*c*) D. A. Rees and W. E. Scott, *J. Chem. Soc. B*, 1971, 469–479.
7 (*a*) M. Poláková, M. U. Roslund, F. S. Ekholm, T. Saloranta and R. Leino, *Eur. J. Org. Chem.*, 2009, 870–888; (*b*) F. S. Ekholm, M. Poláková, A. J. Pawłowicz and R. Leino, *Synthesis*, 2009, 567–576.
8 For a more detailed discussion on the mechanism, see: (*a*) D. Crich and N. S. Chandrasekera, *Angew. Chem., Int. Ed.*, 2004, **43**, 5386–5389; (*b*) D. Crich and S. Sun, *J. Org. Chem.*, 1997, **62**, 1198–1199.
9 See, for example: (*a*) R. V. Stick, *Carbohydrates: The Sweet Molecules of Life*, Academic Press, London, 2001, pp. 179–183; (*b*) G.-J. Boons and K. J. Hale, *Organic Synthesis with Carbohydrates*, Sheffield Academic Press, Sheffield, 2000, pp. 131–135.
10 For a more detailed discussion on the synthesis of compounds **1** and **2**, and the NMR spectroscopic characterization of the building blocks, see ref. 7.
11 For experimental details, see the Experimental section.
12 (*a*) D. Crich and S. Sun, *Tetrahedron*, 1998, **54**, 8321–8348; (*b*) K. Bock and H. Thøgersen, in *Annual Reports on NMR Spectroscopy*, ed. G. A. Webb, Academic Press–Elsevier, London, 1982, pp. 2–49; (*c*) K. Bock and C. Pedersen, *J. Chem. Soc., Perkin Trans. 2*, 1974, 293–299.
13 *NMR Spectroscopy of Glycoconjugates*, ed. J. Jiménez-Barbero and T. Peters, Wiley-VCH, Weinheim, 2003.
14 See for example: (*a*) J. B. Lambert and E. P. Mazzola, *Nuclear Magnetic Resonance Spectroscopy: An Introduction to Principles, Applications and Experimental Methods*, Prentice Hall, New Jersey, 2004, pp. 270–271; (*b*) S. Berger and S. Braun, *200 and More NMR Experiments*, Wiley-VCH, Weinheim, 1998, pp. 488–491.
15 (*a*) R. Laatikainen, M. Niemitz, U. Weber, J. Sundelin, T. Hassinen and J. Vepsäläinen, *J. Magn. Reson., Ser. A*, 1996, **120**, 1–10; (*b*) For detailed information on the software, see: http://www.perchsolutions.com.
16 See, for example: C. J. Cramer, *Essentials of Computational Chemistry: Theories and Models*, Wiley & Sons, Chichester, 2002.
17 See, for example: S. I. van Kasteren, H. B. Kramer, D. P. Gamblin and B. G. Davis, *Nat. Protoc.*, 2007, **2**, 3185–3194.
18 M. J. Frisch, G. W. Trucks, H. B. Schlegel, G. E. Scuseria, M. A. Robb, J. R. Cheeseman, J. A. Montgomery, Jr., T. Vreven, K. N. Kudin, J. C. Burant, J. M. Millam, S. S. Iyengar, J. Tomasi, V. Barone, B. Mennucci, M. Cossi, G. Scalmani, N. Rega, G. A. Petersson, H. Nakatsuji, M. Hada, M. Ehara, K. Toyota, R. Fukuda, J. Hasegawa, M. Ishida, T. Nakajima, Y. Honda, O. Kitao, H. Nakai, M. Klene, X. Li, J. E. Knox, H. P. Hratchian, J. B. Cross, V. Bakken, C. Adamo, J. Jaramillo, R. Gomperts, R. E. Stratmann, O. Yazyev, A. J. Austin, R. Cammi, C. Pomelli, J. Ochterski, P. Y. Ayala, K. Morokuma, G. A. Voth, P. Salvador, J. J. Dannenberg, V. G. Zakrzewski, S. Dapprich, A. D. Daniels, M. C. Strain, O. Farkas, D. K. Malick, A. D. Rabuck, K. Raghavachari, J. B. Foresman, J. V. Ortiz, Q. Cui, A. G. Baboul, S. Clifford, J. Cioslowski, B. B. Stefanov, G. Liu, A. Liashenko, P. Piskorz, I. Komaromi, R. L. Martin, D. J. Fox, T. Keith, M. A. Al-Laham, C. Y. Peng, A. Nanayakkara, M. Challacombe, P. M. W. Gill, B. G. Johnson, W. Chen, M. W. Wong, C. Gonzalez and J. A. Pople, *GAUSSIAN 03 (Revision E.01)*, Gaussian, Inc., Wallingford, CT, 2004.